Chemical Science

ROYAL SOCIETY OF CHEMISTRY

EDGE ARTICLE

View Article Online
View Journal | View Issue

Cite this: *Chem. Sci.*, 2025, **16**, 18936

All publication charges for this article have been paid for by the Royal Society of Chemistry

Received 4th February 2025
Accepted 5th September 2025

DOI: 10.1039/d5sc00912j

rsc.li/chemical-science

Pd-catalyzed desulfonylative fluorination of electron-deficient (hetero)aryl sulfonyl fluorides

Jonathan R. Hall, [a] Natalie P. Romer, [b] Taylor E. Spiller, [a] Matthew S. Sigman [b] and Melanie S. Sanford *[a]

A new C(sp^2)–F bond forming reaction that eliminates the need for exogenous metal fluoride salts is reported. Pd catalysis is used to convert electron-deficient (hetero)aryl sulfonyl fluorides ($ArSO_2F$) to the corresponding (hetero)aryl fluorides with extrusion of SO_2. Data science methods are employed to assess substrate requirements and identify a non-intuitive class of phosphine ligands for this transformation.

Fluorinated molecules are ubiquitous in modern drug discovery since fluorine substituents can be incorporated to modulate biological properties while minimally impacting 3D structure.[1] Currently, approximately 20% of FDA-approved pharmaceuticals contain at least one fluorine atom.[1] Among these, the largest class consists of (hetero)aryl fluorides (ArF), (hetero) aromatic rings bearing at least one C(sp^2)–F bond.[1] Despite the prevalence of the ArF motif, these structures remain challenging to access synthetically.[2,3]

Two of the most common routes to ArF involve reactions of (hetero)aryl halides with a fluoride source: (i) nucleophilic aromatic substitution (S_NAr; Fig. 1a(i))[4,5] and (ii) palladium-catalyzed cross-coupling (Pd catalysis, Fig. 1a(ii)).[6] These transformations are effective for accessing a moderate scope of (hetero)aryl fluoride products, but they share three key limitations. First, both require an excess of an anhydrous fluoride salt (MF), most commonly CsF, KF, AgF, or NMe_4F. These salts are notoriously moisture-sensitive,[7] poorly soluble in organic solvents,[8] and strongly basic.[5,6] As such, reactions involving MF typically require rigorously anhydrous conditions and display modest functional group compatibility. Second, the (hetero)aryl halide starting materials and ArF products often have very similar physical properties and polarities. As such, the separation of ArF from unreacted ArX can be challenging. Finally, benzyne formation[6,9] and protodehalogenation[4] are common side reactions that limit yields and further complicate product purification. The former occurs *via* deprotonation of an *ortho*-C(sp^2)–H bond by the highly basic anhydrous MF, while the latter can derive from slow halide exchange between Pd^{II}(Ar)(X) and MF, which enables competing protonation of the Pd^{II}–Ar bond. Overall, new approaches are required to circumvent these limitations.[10–12]

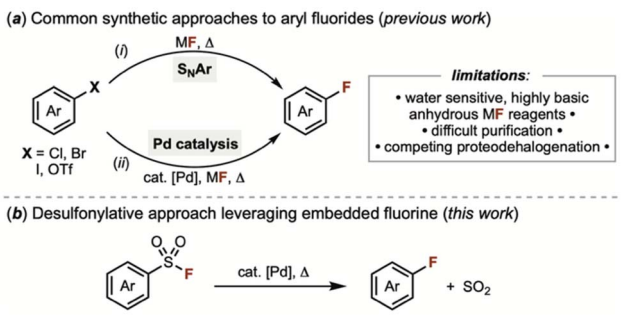

Fig. 1 (a) Literature approaches to ArF. (b) Desulfonylative approach (this work).

We hypothesized that these challenges could be addressed by exploiting (hetero)arene starting materials that contain embedded fluorine. Specifically, we reasoned that (hetero)aryl sulfonyl fluorides ($ArSO_2F$), molecules that are widely available and commonly used as sulfur–fluoride exchange (SuFEx) click chemistry reagents[13,14] could serve as both the electrophile and fluoride source for an intramolecular Pd-catalyzed desulfonylative fluorination (Fig. 1b). This approach offers the advantages that it: (i) avoids the use of strongly basic and water-sensitive MF fluoride salts in the C(sp^2)–F coupling step; (ii) leverages polar starting materials that are readily separable from the non-polar ArF products; and (iii) eliminates the often-problematic halide exchange step from the catalytic cycle.[15]

This report describes the successful development of a Pd-catalyzed desulfonylative fluorination. The transformation is optimized using the commercial sulfonyl fluoride PyFluor[16] and then successfully applied to a variety of electron-deficient heteroaryl sulfonyl fluorides. Data science tools are leveraged to analyze the substrate requirements for effective reaction as well as to identify a novel class of phosphine ligands for this Pd-catalyzed C(sp^2)–F coupling.

[a]*Department of Chemistry, University of Michigan Ann Arbor, 930 North University Avenue, Ann Arbor, MI 48109, USA. E-mail: mssanfor@umich.edu*

[b]*Department of Chemistry, University of Utah, 315 1400 E, Salt Lake City, UT 84112, USA*

We started by considering a putative catalytic cycle for desulfonylative fluorination inspired by literature precedent for each of the individual steps (Fig. 2).[17] We envisioned that initial oxidative addition of $ArSO_2F$ at Pd^0 could generate $Pd^{II}(Ar)(SO_2F)$ intermediate **A** (step i), which could then undergo SO_2 deinsertion to form $Pd^{II}(Ar)(F)$ complex **B** (step ii).[18–20] The feasibility of steps i and ii has been established in other Pd-catalyzed cross-coupling reactions of sulfonyl fluorides.[18–20] Notably, **B** is also an intermediate in Pd-catalyzed fluorinations with ArX starting materials, but in those systems it is formed *via* an often-challenging halide exchange between $Pd^{II}(Ar)(X)$ and MF.[8–10] Finally, Ar–F bond-forming reductive elimination (step iii) would release the product and regenerate the Pd^0 catalyst.[17] Prior work has shown that this elementary step is feasible with a narrow set of sterically demanding *ortho*-biaryl monophosphine ligands (*e.g.*, BrettPhos, *t*BuBrettPhos, AdBrettPhos, and AlPhos; Table 1).[17]

Reaction development and optimization were initiated using PyFluor (Table 1, **1a**) as a model substrate.[16] **1a** was selected as a starting point based on its commercial availability as well as its known reactivity towards Ar–SO_2F oxidative addition in several related Pd-catalyzed desulfonylative cross-coupling reactions.[18–20] A first set of experiments was performed using BrettPhos, a reported ligand for Ar–F coupling reactions,[6] and Pd_2dba_3, a common source of Pd^0. In toluene at 150 °C, the Pd^0/Brettphos catalyst afforded the desulfonylative fluorination product 2-fluoropyridine (**2a**) in 14% yield (Table 1, entry 1). Other ligands known to promote Ar–F coupling, including AdBrettPhos, AlPhos, and *t*BuBrettPhos, proved even more effective, providing 76–83% yield of **2a** (entries 2–4). In contrast, XPhos, SPhos, and RuPhos afforded <5% product (entries 6–8). After evaluating various conditions, we identified Pd_2dba_3 (5 mol%) and *t*BuBrettPhos (20 mol%) in toluene (0.2 M for screening scale, 0.33 M for isolation scale) at 150 °C for 18 h as optimized conditions (Table 1, entry 4). A noteworthy feature of this transformation is that, unlike fluorinations employing moisture-sensitive MF reagents, it does not require rigorously anhydrous conditions. Setting the desulfonylative fluorination of **1a** up on the benchtop using off-the-shelf toluene (0.1 M, deoxygenated with a purge of N_2) led to 77% yield of 2-fluoropyridine (entry 5) in 4 h. Furthermore, conducting the analogous reaction under air without any precautions towards air or moisture (entry 7) afforded **2a** in 71% yield. These yields are comparable to those for reactions set up in the glovebox in dry toluene (entries 4 and 5).

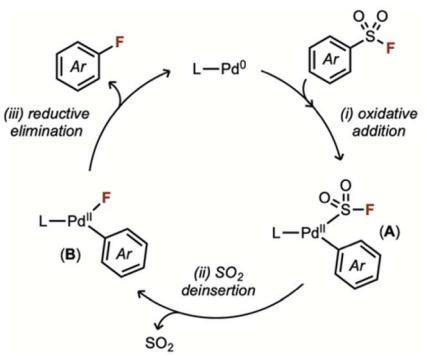

Fig. 2 Potential $Pd^{0/II}$ catalytic cycle for desulfonylative fluorination.

We next explored the scope of heteroaryl sulfonyl fluorides that participate in Pd-catalyzed desulfonylative fluorination (Fig. 3). Various 2-substituted pyridine, pyrimidine, pyrazine, and quinoline sulfonyl fluorides reacted to afford the corresponding ArF products (**2a–n**) in good yields under the optimized conditions. The 4-substituted quinoline sulfonyl fluoride showed minimal reactivity at 150 °C, but raising the temperature to 160 °C resulted in a 56% yield of **2j** after 24 h. Pyridines bearing sulfonyl fluoride substituents at the less activated 3-position afforded <5% aryl fluoride under the optimized conditions (see Scheme S2), returning unreacted starting material.

To evaluate functional group compatibility, a series of biarylpyridine sulfonyl fluorides were examined (Fig. 3). This series afforded >60% yield for substrates containing benzofuran, benzothiophene, and tertiary aniline substituents (products **2t**, **2u**, **2x**). In addition, both enolizable ketones (**2y**) and aromatic aldehydes (**2za**) were well-tolerated. Analogues containing an *N*-methylindole (**2v**) and a Boc-protected aniline (**2zb**) afforded low yields (23% and 12%, respectively). The former is largely due to poor solubility in the reaction medium, while the latter showed low conversion of the starting sulfonyl fluoride. Several functional groups proved incompatible, including silyl protected phenols (which appear to undergo deprotection under the reaction conditions) as well as nitro and unprotected aniline substituents (see Scheme S2 for details). A series of purines underwent desulfonylative fluorination on the 6-membered ring in moderate to good yield (products **2k–2n**). Finally, a triazole derivative was also an effective substrate, affording the corresponding ArF (**2o**) in 83% isolated yield. Five-membered heterocycles are a notoriously challenging class of substrates for Pd-catalyzed aryl halide fluorination reactions with MF.[15]

Protodesulfonylated products were generally not detected by HPLC or GCMS analysis of the crude reaction mixtures. This, in combination with the large polarity difference between $ArSO_2F$ and ArF, made purification/isolation straightforward for most non-volatile products. The crude reaction mixtures were filtered through a plug of silica, evaporated to dryness, and then subjected to a single round of column chromatography on silica gel to afford ArF in >95% purity. The heteroaryl fluoride products could also be carried forward *in situ* to S_NAr reactions. For instance, a telescoped one-pot sequence was used to convert pyrimidine-2-sulfonyl fluoride into the corresponding ether-, aniline-, and cyano-substituted pyrimidine products (Fig. 4).

Aryl sulfonyl fluorides bearing electron-withdrawing substituents (CN, CO_2Me, CF_3) were next evaluated. These substrates all afforded <10% yield of products **2p–s** under the conditions optimized for substrate **1a**. Changing the ligand to BrettPhos and the solvent to cyclohexane resulted in improved yields of 2-fluorobenzonitrile (**2p**, 56%) and 4-fluorobenzonitrile (**2q**, 60%). However, even under these modified conditions, low reactivity was observed for the 2-CO_2Et derivative; furthermore, the 4-CF_3 substrate returned only trace

Table 1 Optimization of desulfonylative fluorination with model substrate **1a**

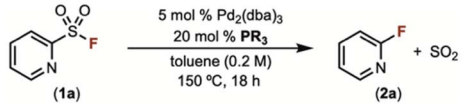

Entry	Phosphine	Modifications	Yield **2a** (conversion)
1	BrettPhos	None	14% (62%)
2	AdBrettPhos	None	78% (100%)
3	AlPhos	AlPhosPd$_2$COD as precatalyst	76% (94%)
4	*t*BuBrettPhos	None	83% (100%)
5	*t*BuBrettPhos	Glovebox, dry toluene, 4 h, 0.1 M	64% (100%)
6	*t*BuBrettPhos	Benchtop, off-the-shelf toluene, 4 h, 0.1 M, N_2 purge before heating	77% (100%)
7	*t*BuBrettPhos	Benchtop, off-the-shelf toluene, 4 h, 0.1 M, in ambient air	71% (85%)
8	XPhos	None	<5% (40%)
9	SPhos	None	<5% (43%)
10	RuPhos	None	<5% (42%)
11	*t*BuBrettPhos	In cyclohexane	59% (100%)
12	*t*BuBrettPhos	In 2-MeTHF	21% (67%)
13	*t*BuBrettPhos	No [Pd]	0% (0%)
14	—	No phosphine	0% (0%)

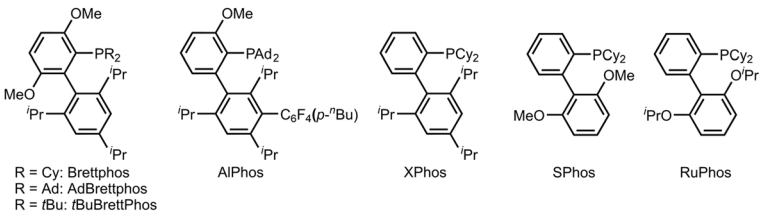

product along with a complex mixture of side products and unreacted starting material. The requirement for a strongly electron-withdrawing substituent is a common limitation of Pd-catalyzed cross-couplings of (hetero)arylsulfonyl fluorides and is typically rationalized based on slow rates of Ar–S oxidative addition with more electron-rich substrates.†[18,20]

We pursued data science studies to establish a simple and quantitative metric that predicts substrate reactivity in this transformation. A single-node decision tree was used to classify (hetero)aryl sulfonyl fluoride substrates above and below a threshold of 25% yield (Fig. 5A).[21] These data were divided into training, validation, and external test sets, and a good

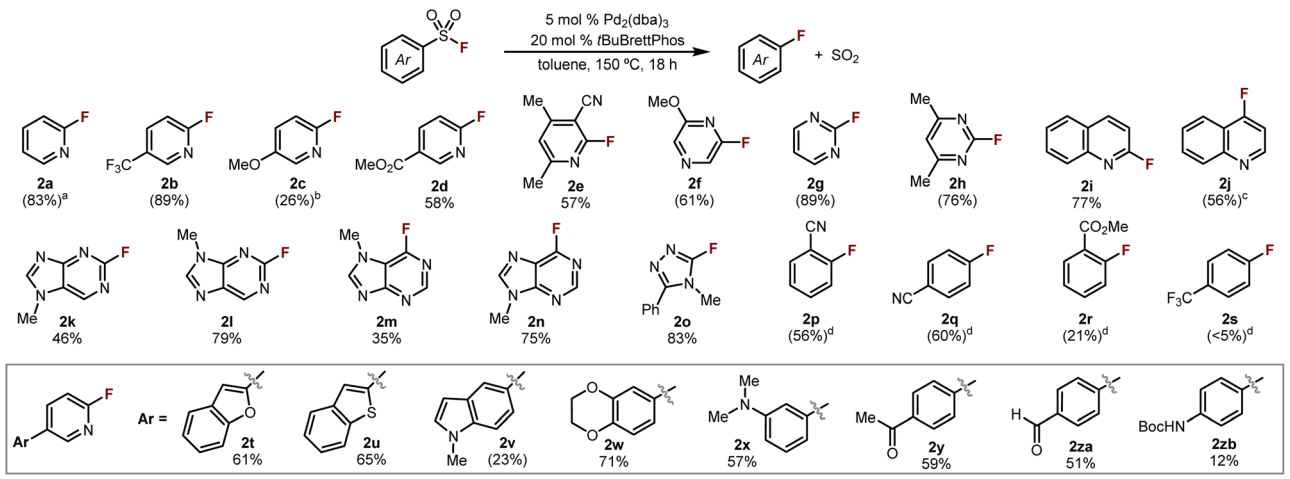

Fig. 3 Substrate scope of desulfonylative fluorination. Isolation scale reactions performed on 0.3 mmol scale in toluene (0.33 M) with Pd$_2$(dba)$_3$ (5 mol%) and *t*BuBrettPhos (20 mol%) for 18 h at 150 °C. Yields in parentheses correspond to crude yields obtained by ^{19}F NMR spectroscopy or HPLC. See SI Scheme S1 for details on products that were not isolated. [a] 4 h. [b] AdBrettPhos (10 mol%)/cyclohexane. [c] Reaction performed at 160 °C. [d] BrettPhos (20 mol%)/cyclohexane.

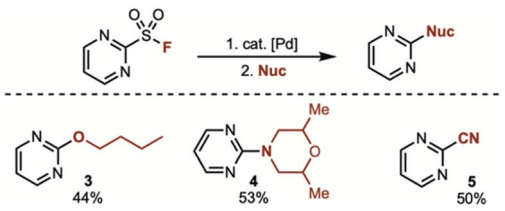

Fig. 4 Sequential desulfonylative fluorination/S_NAr.

classification [test accuracy = 0.87] was identified with the C(sp^2)–S bond length (Å), where substrates with longer C–S bonds afforded higher yields. We hypothesize that this descriptor is reporting on the first step of the catalytic cycle – oxidative addition – with longer C(sp^2)–S bonds being more reactive.[18] Notably, the triazole (**2o**) was the sole outlier in the external test set, likely because it is the only 5-membered heterocycle included in this study (Fig. 5A). Without additional training data for 5-membered sulfonyl fluorides, the current model may be limited to predicting the reactivity of 6-membered heterocycle substrates.[18,20]

Finally, we sought to identify new ligand scaffolds for this Pd-catalyzed desulfonylative fluorination. Despite more than 30 years of literature studies,[17,22] only a narrow set of biaryl-substituted phosphines (BrettPhos derivatives and AlPhos) have been reported to enable Ar–F coupling at Pd^{II}.[17,23] Our initial screen of 11 ligands identified several additional biaryl phosphines [RockPhos (63%), Me_3MeO*t*BuXPhos (61%)] that promote the desulfonylative fluorination of PyFluor, albeit in lower yield than *t*BuBrettPhos (83%). We evaluated correlations between reaction yield and computed phosphine ligand structural descriptors (from the kraken database) of this sparse training set (Fig. 5B). Despite the limited data set and low coverage of chemical space, we sought to leverage simple models to guide screening of new phosphines for this transformation. The eleven monophosphines were analyzed against DFT-computed molecular descriptors from the kraken monophosphine descriptor library.[24] Three univariate correlations (minimum buried volume, phosphorus lone pair orbital energy, and pyramidalization[25]) were identified that correctly group the high activity (>25% yield) and low activity (<25% yield) ligands (Fig. 5C).

The kraken monophosphine descriptor library was next curated to ~300 commercially available phosphine ligands and queried to identify either interpolations (referred to as the "explore" region) or extrapolations (referred to as the "exploit" region) based on descriptor values from the preliminary

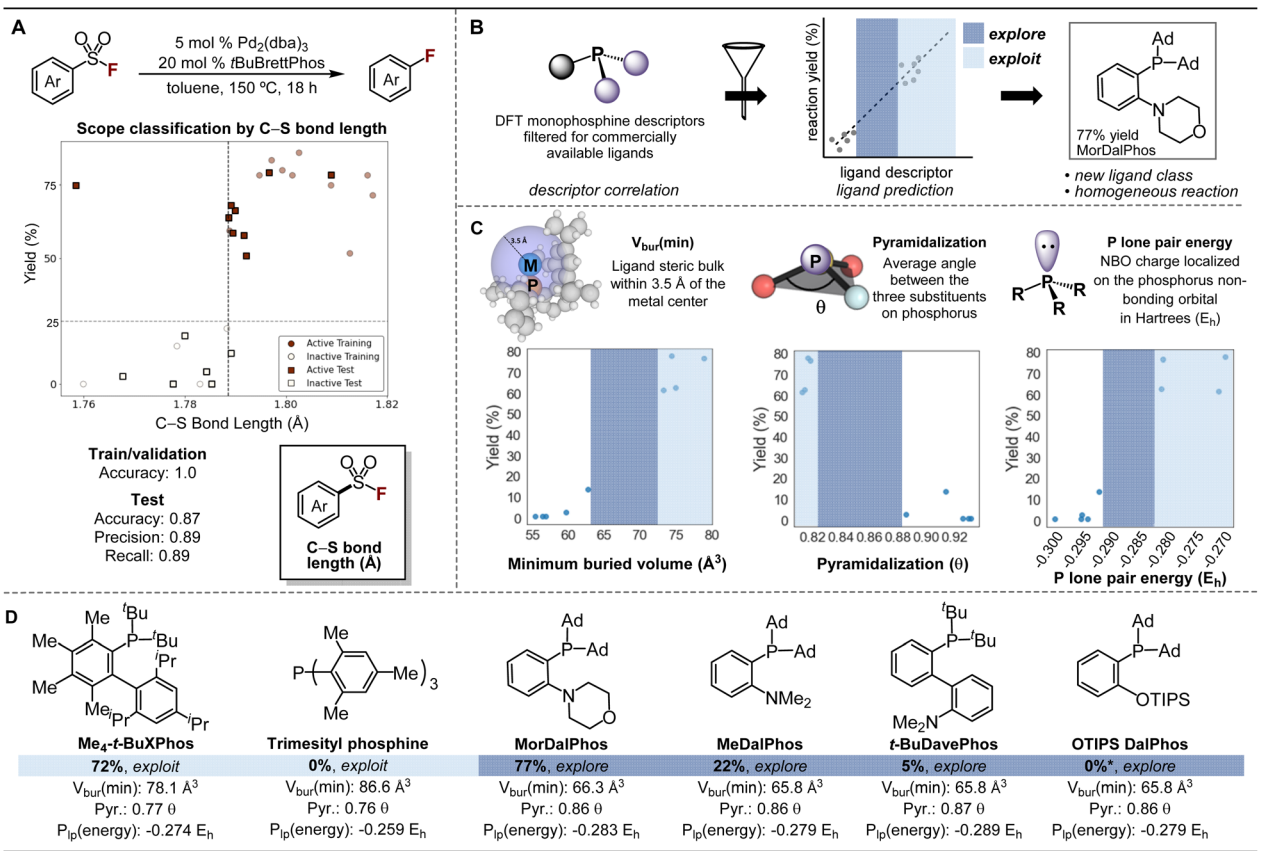

Fig. 5 (A) Single node decision tree (25% yield threshold) of the heteroaryl sulfonyl fluoride scope with the C–S bond length (Å). We hypothesize longer, weaker C–S bonds (>1.789 Å) more readily undergo oxidative addition. (B) Data science workflow for ligand structure–activity analysis and prediction. (C) Univariate ligand descriptor correlations with training set data. (D) Examples of predicted ligands from explore and exploit regions with relevant molecular descriptor values.

models, as well as availability and cost (Fig. 5C). Specifically, this involved 'exploring' ligands with descriptor values that were untested in the training set, and 'exploiting' ligands with descriptor values correlated to high yield. Ten total ligands were selected from the 'explore' and 'exploit' regions of all three preliminary correlations and tested against substrate **1a** (see SI Section VII). This led to the identification of several new ligands for the desulfonylative fluorination of PyFluor (Fig. 5D). For instance, Me$_4$*t*BuXPhos, which is structurally similar to Me$_3$-MeO*t*BuXPhos, afforded a comparable 72% yield of 2-fluoropyridine. In contrast, trimesitylphosphine was inactive in the reaction, despite being classified in the 'exploit' region. While trimesitylphosphine replicates the steric bulk of *ortho*-biaryl phosphines, it lacks electron donating alkyl substituents on phosphorus and does not contain an *ipso*-biaryl carbon center to enable dative bidentate coordination to the metal center. Unexpectedly, MeDalPhos (22% yield) and MorDalPhos (77% yield, Fig. 5D), phosphines that do not contain biaryl linkages and are commonly considered P,N-bidentate ligands, were active in this reaction.[26] Moreover, in marked contrast to the *t*BuBrettPhos system that generates a large amount of precipitate as the reaction progresses, MorDalPhos leads to a homogeneous solution throughout the 18 h reaction time course.

Overall, the use of data science to analyze the ligand structure–activity relationship enabled the identification of a new structural class of ligands for Pd-catalyzed Ar–F coupling. While MorDalPhos does not offer major improvements in terms of reaction yield or substrate scope, the success of this scaffold offers new chemical space for ligand innovation moving forward. In addition, the homogeneity of reactions with this ligand (compared to the heterogeneous mixtures with *t*BuBrettPhos) offers potential advantages for scaling these transformations. Future efforts will involve organometallic studies to compare the structure and reactivity of putative catalyst intermediates with these new ligands.

Conclusions

Overall, this report presents a novel approach to (hetero)aryl fluoride synthesis that leverages a fluoride-containing substrate as an internal fluoride source. Accessing the key LPd(Ar)(F) intermediate *via* oxidative addition/SO_2 deinsertion rather than halide exchange eliminates the need for exogenous fluoride. Key advantages of this approach include enhanced water tolerance, minimal formation of side products, and straightforward purification of the ArF products. Data science studies have identified Ar–S bond distance as a simple metric for predicting $ArSO_2F$ substrate reactivity for 6-membered ring (hetero) aromatic substrates. Additionally, through data science analysis of ligand effects, MeDalPhos and MorDalPhos were identified as phosphine ligands for promoting Pd-catalyzed desulfonylative fluorination. Ongoing work is focused on organometallic studies to interrogate key intermediates and understand ligand effects on the rates of each step of the proposed catalytic cycle. Additionally, we aim to apply this approach to other starting materials that contain embedded fluorine (*e.g.*, (hetero) aryl acid fluorides).

Author contributions

The project was conceptualized by J. R. H. and M. S. Sanford. Experimental work was conducted by J. R. H. and T. E. S. All data science and statistical analyses were conducted by N. P. R. in conjunction with M. S. Sigman. Manuscript drafts were written by J. R. H., T. E. S., and M. S. Sanford, with review and editing by all authors. Funding acquisition was led by M. S. Sanford and M. S. Sigman. The project was supervised by M. S. Sanford and M. S. Sigman.

Conflicts of interest

There are no conflicts to declare.

Data availability

Details concerning the data science techniques applied in this report can be found at: **https://github.com/SigmanGroup/Desulfonylative_Fluorination**. Coordinates for the data science applications can be found in an attached xyz file.

Supplementary information: Detailed experimental protocols and characterization data for novel compounds. See DOI: **https://doi.org/10.1039/d5sc00912j**.

Acknowledgements

This work was supported by NIH NIGMS (R35GM1361332 to M. S. Sanford). Researchers in the Sigman Lab acknowledge financial support from the NSF under the CCI Center for Computer Assisted Synthesis (CHE-2202693 to M. S. Sigman). Support and resources from the Center for High Performance Computing at the University of Utah are gratefully acknowledged.

Notes and references

† While the ligand effects observed in this system are consistent with an inner-sphere reductive elimination, we acknowledge the possibility of a non-traditional S_NAr-type reductive elimination as described in ref. 23, in line with the requirement for strongly electron-deficient substrates.

1 M. Inoue, Y. Sumii and N. Shibata, *ACS Omega*, 2020, **5**, 10633–10640.
2 D. E. Yerien, S. Bonesi and A. Postigo, *Org. Biomol. Chem.*, 2016, **14**, 8398–8427.
3 S. Caron, *Org. Process Res. Dev.*, 2020, **24**, 470–480.
4 S. D. Schimler, S. J. Ryan, D. C. Bland, J. E. Anderson and M. S. Sanford, *J. Org. Chem.*, 2015, **80**, 12137–12145.
5 C. M. Hong, A. M. Whittaker and D. M. Schultz, *J. Org. Chem.*, 2021, **86**, 3999–4006.
6 D. A. Watson, M. Su, G. Teverovskiy, Y. Zhang, J. García-Fortanet, T. Kinzel and S. L. Buchwald, *Science*, 2009, **325**, 1661–1664.
7 M. T. Morales-Colón, Y. Y. See, S. J. Lee, P. J. H. Scott, D. C. Bland and M. S. Sanford, *Org. Lett.*, 2021, **23**, 4493–4498.

8 Y. Y. See, M. T. Morales-Colon, D. C. Bland and M. S. Sanford, *Acc. Chem. Res.*, 2020, **53**, 2372–2383.
9 A. C. Sather, H. G. Lee, V. Y. De La Rosa, Y. Yang, P. Muller and S. L. Buchwald, *J. Am. Chem. Soc.*, 2015, **137**, 13433–13438.
10 Several reports describe the deoxyfluorination of phenols:(*a*) P. Tang, W. Wang and T. Ritter, *J. Am. Chem. Soc.*, 2011, **133**, 11482–11484; (*b*) S. D. Schimler, M. A. Cismesia, P. S. Hanley, R. D. J. Froese, M. J. Jansma, D. C. Bland and M. S. Sanford, *J. Am. Chem. Soc.*, 2017, **139**, 1452–1455.
11 Cu-mediated fluorination of (hetero)aryl-boron derivatives with MF is another common approach. However, these transformations suffer from similar challenges, including moisture sensitive fluoride sources, competing formation of ArH, and challenging purifications:(*a*) Y. Ye, S. D. Schimler, P. S. Hanley and M. S. Sanford, *J. Am. Chem. Soc.*, 2013, **135**, 16292–16295; (*b*) T. Furuya, H. M. Kaiser and T. Ritter, *Angew. Chem., Int. Ed.*, 2008, **47**, 5993–5996; (*c*) P. S. Fier, J. Luo and J. F. Hartwig, *J. Am. Chem. Soc.*, 2013, **135**, 2552–2559.
12 Cu-mediated radical based nucleophilic fluorination sequences are also emerging. Again, the use of MF, the formation of ArH, and purification remain challenges:(*a*) P. Xu, P. Lopez-Rojas and T. Ritter, *J. Am. Chem. Soc.*, 2021, **143**, 5349–5354; (*b*) T. Q. Chen, P. S. Pedersen, N. W. Dow, R. Fayad, C. E. Hauke, M. C. Rosko, E. O. Danilov, D. C. Blakemore, A.-M. Dechert-Schmitt, T. Knauber, F. N. Castellano and D. W. C. MacMillan, *J. Am. Chem. Soc.*, 2022, **144**, 8296–8305; (*c*) T. E. Spiller, K. Donabauer, A. F. Brooks, J. A. Witek, G. D. Bowden, P. J. H. Scott and M. S. Sanford, *Org. Lett.*, 2024, **26**, 6433–6437.
13 J. Dong, L. Krasnova, M. G. Finn and K. B. Sharpless, *Angew Chem. Int. Ed. Engl.*, 2014, **53**, 9430–9448.
14 S. W. H. Wright and N. Kelly, *J. Org. Chem.*, 2006, **71**(3), 1080–1084.
15 H. G. Lee, P. J. Milner and S. L. Buchwald, *J. Am. Chem. Soc.*, 2014, **136**, 3792–3795.
16 M. K. Nielsen, C. R. Ugaz, W. Li and A. G. Doyle, *J. Am. Chem. Soc.*, 2015, **137**, 9571–9574.
17 A. C. Sather and S. L. Buchwald, *Acc. Chem. Res.*, 2016, **49**, 2146–2157.
18 P. Chatelain, C. Muller, A. Sau, D. Brykczyńska, M. Bahadori, C. N. Rowley and J. Moran, *Angew. Chem., Int. Ed.*, 2021, **60**, 25307–25312.
19 G. Zhang, C. Guan, Y. Zhao, H. Miao and C. Ding, *New J. Chem.*, 2022, **46**, 3560–3564.
20 J. Rueda-Espinosa, D. Ramanayake, N. D. Ball and J. A. Love, *Can. J. Chem.*, 2023, **101**, 765–772.
21 S. H. Newman-Stonebraker, S. R. Smith, J. E. Borowski, E. Peters, T. Gensch, H. C. Johnson, M. S. Sigman and A. G. Doyle, *Science*, 2021, **374**, 301–308.
22 V. V. Grushin, *Acc. Chem. Res.*, 2010, **43**, 160–171.
23 V. V. Grushin and W. J. Marshall, *Organometallics*, 2007, **26**, 4997–5002.
24 T. Gensch, G. dos Passos Gomes, P. Friederich, E. Peters, T. Gaudin, R. Pollice, K. Jorner, A. Nigam, M. Lindner-D'Addario, M. S. Sigman and A. Aspuru-Guzik, *J. Am. Chem. Soc.*, 2022, **144**, 1205–1217.
25 T. P. Radhakrishnan and I. Agranat, *Struct. Chem.*, 1991, **2**, 107–115.
26 R. J. Lundgren, B. D. Peters, P. G. Alsabeh and M. Stradiotto, *Angew. Chem., Int. Ed.*, 2010, **49**, 4071–4074.